Yu et al. *Zool. Res.* 2026, 47(6): 1941−1956
https://doi.org/10.24272/j.issn.2095-8137.2025.633
https://cstr.cn/32248.14.zr.2025.633

ZR | Zoological Research

Article Open Access

DAPK3 activates STING to enhance antiviral response via IRF3 and NF-κB pathways in teleosts

Ting-Ting Yu[1], Cheng-Yu Hu[1], Quan-Ling Zhang[1], Miao-Miao Li[1], Chen Guo[1], Mei-Feng Li[2], Li-Hua Fan[1], Shang-Hong Wang[1], Hui-Ling Mao[1], Dong-Ming Li[3], Ze-Yin Jiang[4,*], Xiao-Wen Xu[1,*]

[1] *School of Life Science*, *Nanchang University*, *Nanchang* 330031, *Jiangxi*, *China*

[2] *Institute of Pathogenic Microorganism and College of Bioscience and Engineering*, *Jiangxi Agricultural University*, *Nanchang*, *Jiangxi* 330045, *China*

[3] *Fuzhou Medical College*, *Nanchang University*, *Fuzhou*, *Jiangxi* 344000, *China*

[4] *College of Food Science and Technology*, *Nanchang University*, *Nanchang*, *Jiangxi* 330039, *China*

ABSTRACT

Stimulator of interferon genes (STING) is critical for the induction of type I interferons (IFN-I) and inflammatory responses against viral infection. The activity of STING is tightly regulated by various post-translational modifications (PTMs) to effectively defend against viral infection or prevent excessive immune responses. However, the regulatory mechanisms of STING activity remain largely unknown in teleosts. In this study, we discovered that zebrafish death-associated protein kinase 3 (DAPK3) enhances the STING-mediated antiviral innate immune response through two synergistic mechanisms: the induction of an interferon regulatory factor 3 (IRF3)-dependent IFN-I response and a nuclear factor kappa B (NF-κB)-dependent pro-inflammatory cytokine response. Specifically, viral stimulation triggers the expression of DAPK3, resulting in its autophosphorylation at Ser21 and Thr87. Activated DAPK3 subsequently interacts with STING, promoting its phosphorylation. Moreover, DAPK3 also recruits tripartite motif-containing protein 32 (TRIM32), an E3 ubiquitin ligase, thereby increasing K63-linked polyubiquitination of STING. Subsequently, activated STING orchestrates two key responses: (i) it recruits TBK1 to enhance IRF3 phosphorylation and dimerization, thereby promoting IFN-I production; (ii) it recruits the IKK complex (IKKα/IKKβ) to activate p65-mediated expression of pro-inflammatory cytokines (IL-6, IL-1β, TNFα), ultimately inducing apoptosis. At the cellular level, DAPK3 overexpression significantly enhances cellular antiviral capacity and inhibits viral proliferation. *In vivo*, zebrafish embryos injected with DAPK3 mRNA display reduced lethality and decreased viral mRNA levels compared to controls. This is accompanied by the induction of immune-related genes and pro-inflammatory cytokines. Conversely, knocking down DAPK3 in zebrafish enhances spring viremia of carp virus (SVCV)-induced lethality and viral proliferation, a phenomenon associated with a reduction in immune-related genes and pro-inflammatory cytokines. Collectively, these findings underscore the critical role of zebrafish DAPK3 in enhancing the antiviral response through two synergistic mechanisms that target STING.

Keywords: DAPK3; STING; Phosphorylation; Antiviral response; Ubiquitination

INTRODUCTION

The innate immune response serves as the primary host defense against invading pathogens and danger signals, initiated by a diverse array of pattern recognition receptors (PRRs) (Kawai & Akira, 2006; Topham et al., 2024; Zhang et al., 2023a). These PRRs, including toll-like receptors (TLRs), retinoic acid-inducible gene I (RIG-I)-like receptors (RLRs), NOD-like receptors (NLRs), and cytosolic DNA receptors, are activated upon recognition of conserved pathogen-associated molecular patterns (PAMPs) (Ru et al., 2025; Creagh & O'Neill, 2006; Shu & Wang, 2014; Takeuchi & Akira, 2010). This recognition promptly triggers innate immune signaling pathways, such as the production of interferon (IFN), activation of nuclear factor kappa B (NF-κB), and the release of inflammatory cytokines (Su, 2025). Notably, many PRRs, including cGAS and DAI, efficiently initiate the innate immune response via the adaptor protein STING (Pan et al., 2023; Du & Chen, 2018; Takaoka et al., 2007). Consequently, STING plays a central role in orchestrating the innate immune response against viral and bacterial infections.

This is an open-access article distributed under the terms of the Creative Commons Attribution Non-Commercial License (http://creativecommons.org/licenses/by-nc/4.0/), which permits unrestricted non-commercial use, distribution, and reproduction in any medium, provided the original work is properly cited.

Copyright ©2026 Editorial Office of Zoological Research, Kunming Institute of Zoology, Chinese Academy of Sciences

Received: 03 March 2026; Accepted: 15 April 2026; Online: 16 April 2026

Foundation items: This work was supported by the National Natural Science Foundation of China (32260926, 32460928) and Natural Science Foundation of Jiangxi Province (20242BAB20316, 20243BCE51118)

*Corresponding authors, E-mail: Jiangzy20230915@163.com; xuxw2020@163.com

Post-translational modifications (PTMs) represent the covalent attachment of small chemical groups, often derived from metabolites, to protein macromolecules. These modifications are critical for expanding the functional diversity of the proteome. PTMs are numerous, with over 400 recognized types currently known, including traditional modifications such as phosphorylation, ubiquitination, glycosylation, and acetylation (Yang et al., 2023). PTMs have been shown to influence innate immune responses by modifying receptors, adaptors, transcriptional regulators, and even viral proteins (Kokkinidis et al., 2020). As a key adaptor in innate immunity, STING activity is well-known to be regulated by different PTMs, including phosphorylation, ubiquitination, palmitoylation, and ISGylation (Liu et al., 2015; Qin et al., 2024; Zhang et al., 2020; Zhou et al., 2023).

Death-associated protein kinase 3 (DAPK3), a Ser/Thr protein kinase widely expressed across various tissues, belongs to the Death-Associated Protein Kinase (DAPK) family, which includes five members (DAPK1, DAPK2, DAPK3, DRAK1, and DRAK2) (Das et al., 2016). The DAPK3 protein structure comprises four putative nuclear localization signal sequences, a leucine zipper domain, and a catalytic domain. Specifically, the leucine zipper domain mediates homodimerization and kinase activation (Farag & Roh, 2019). Previous studies have implicated DAPK3 in tumor suppression and autophagy regulation (Cai et al., 2015; Fujiwara et al., 2016; Yang et al., 2025). In addition to these established roles, emerging evidence suggests that DAPK3 is also involved in antiviral and inflammatory responses. The classical swine fever virus (CSFV) NS5A protein activates the PP2A-DAPK3-Beclin 1 axis to favor its replication (Sun et al., 2023). Moreover, DAPK3 can activate the AKT/IκB/NF-κB-mediated inflammatory pathway to promote epithelial-mesenchymal transition (EMT) (Li et al., 2015). Notably, DAPK3 is reported to regulate STING-dependent IFN production (Takahashi et al., 2021). Nevertheless, the precise regulatory mechanisms governing DAPK3 kinase activity, as well as its role in the downstream STING-mediated antiviral pathway, remain to be fully elucidated.

Zebrafish are a well-established model for studying innate immune pathways (Guo et al., 2026). Given that STING in fish, similar to its mammalian counterpart, participates in the regulation of antiviral immunity and inflammatory responses (Qin et al., 2023), we investigated the role of the DAPK3-STING signaling axis in these processes. Our data suggest that viral infection increases the phosphorylation of DAPK3 at Ser21 and Thr87; subsequently, DAPK3 interacts with STING and promotes its phosphorylation. TRIM32 is then recruited by the DAPK3-STING dimer, increasing K63-linked polyubiquitination of STING and thereby enhancing its activation. Activated STING then drives type I IFN (IFN-I) production through interferon regulatory factor 3 (IRF3) activation. Concurrently, STING also targets the IKKα/IKKβ complex to activate NF-κB-dependent induction of inflammatory factors. Our combined in vitro and in vivo experiments demonstrate that zebrafish DAPK3 exhibits potent antiviral activity against spring viremia of carp virus (SVCV) infection through these two synergistic mechanisms targeting STING, highlighting its dual role in coordinating antiviral and inflammatory responses.

MATERIALS AND METHODS

Zebrafish strain and cell lines

Zebrafish (*Danio rerio*) of the AB strain were purchased from Nanjing EzeRinka Biotechnology Co., Ltd, China. The fish were maintained in a recirculating aquaculture system (ESEN, China) according to established protocols. All zebrafish experiments were performed in strict compliance with the Guide for the Care and Use of Laboratory Animals at Nanchang University (IACUC Approval No. NCUAUU-2022-563).

Zebrafish caudal fin (ZFIN) cells were cultured in DMEM medium supplemented with 10% fetal bovine serum (FBS). Epithelioma papulosum cyprini (EPC) cells and grass carp (*Ctenopharyngodon idella*) kidney (CIK) cells were maintained in M199 medium supplemented with 10% FBS and incubated at 28°C in a humidified incubator with 5% CO_2. All cell lines were confirmed to be free of Mycoplasma contamination prior to use.

Viruses and viral analogues

Spring viremia of carp virus (SVCV) was propagated in EPC cells, while grass carp reovirus 873 (GCRV 873) was propagated in grass carp kidney (CIK) cells. Viral supernatant was collected when complete cytopathic effects (CPEs) were observed in the infected cells. Viral titers were determined using the 50% tissue culture infectious dose ($TCID_{50}$) assay. Two viral analogues, B-DNA and Z-DNA, were synthesized by Sangon Biotech (China) and subsequently diluted in deionized (DI) water to achieve a final concentration of 10 μM. Their sequences are provided in Supplementary Table S1.

To detect gene expression in zebrafish tissues, 3-month-old zebrafish were intraperitoneally injected with 10 μL of SVCV (10^4 $TCID_{50}$/mL), GCRV (10^6 $TCID_{50}$/mL), 10 μmol/L B-DNA, or 10 μmol/L Z-DNA. For *in vitro* viral infection experiments, CIK and ZFIN cells cultured in 6-well plates were infected with 10 μL of GCRV and SVCV, respectively. ZFIN cells were also transfected with 2 μg of B-DNA and Z-DNA. Total RNA was extracted from each tissue sample at 6, 12, 24, 48, and 72 hours post-stimulation. Quantitative real-time PCR (qPCR) was performed to detect DAPK3 expression. Control groups were treated with an equivalent volume of PBS.

Plasmid construction and reagents

The zebrafish genes DAPK3 (Gene ID: 562194) and STING (Gene ID: 101243556), along with their truncated mutants, were amplified from cDNA derived from zebrafish tissues using PCR. The amplified gene fragments were then separately cloned into the pCMV-Flag (Clontech, USA), pEGFP-C1 (Clontech, USA), and pcDNA3.1-basic (Clontech, USA) expression vectors. The resulting recombinant plasmids were confirmed by DNA sequencing.

Plasmids were transfected using the Lipo8000™ transfection reagent (Beyotime, China) at a 1:1.2 ratio of DNA (μg) to transfection reagent (μL). Oligonucleotides B-DNA and Z-DNA were transfected using Lipofectamine 2000 (Invitrogen, USA) at a 1:1 ratio of DNA (μg) to transfection reagent (μL). Specific small interfering RNAs (siRNAs) were transfected using the HiPerFect transfection reagent (Qiagen, Germany) at a 1:3 ratio of DNA (μg) to transfection reagent (μL). The antibodies used in this study were as follows: Mouse anti-Flag antibody (Sigma, USA), Mouse anti-GFP antibody (Abmart, China), Rabbit anti-Histone H3 antibody (Affinity, USA), Mouse anti-β-tubulin antibody (Abmart, China), Rabbit anti-DAPK3 antibody (Abmart, China), Rabbit anti-IRF3 and anti-phospho-IRF3 antibodies (Beyotime, China), Anti-TBK1 and anti-phospho-TBK1 antibodies (Affinity, USA), Rabbit pan-phospho-serine/threonine/tyrosine antibody (Abcam, USA),

Goat anti-mouse Alexa Fluor 594-labeled antibody (ZSGB-Bio, China). Rabbit polyclonal anti-IFN-I antisera were prepared in our laboratory (Xu et al., 2017). The product codes of all commercial antibodies are listed in Supplementary Table S2.

qPCR analysis

Total RNA was extracted from tissue, cell, and larval samples using the Total RNA Extraction Kit (Tiangen, China). First-strand cDNA was synthesized from 1 μg of extracted RNA using the Quantscript RT Kit (TaKaRa, Japan). qPCR was performed using TB Green PCR Master Mix (TaKaRa, Japan). The PCR cycling conditions were as follows: an initial denaturation at 95°C for 3 min, followed by 35 cycles of denaturation at 95°C for 30 sec, annealing at 55°C for 30 sec, and extension at 72°C for 30 sec. Gene relative expression levels were calculated using the $2^{-\Delta\Delta CT}$ method. *β-actin* served as the reference gene. The data represent the mean results from three independent experiments, each with technical triplicates. Primers used for qPCR are listed in Supplementary Table S1. The schematic diagrams of experimental design are detailed in Supplementary Figure S1.

Dual-luciferase reporter assay

ZFIN cells were seeded in 6-well plates and co-transfected with the following plasmids: 0.25 μg of pGL3-IFN-I-promoter, 1 μg of DAPK3-pcDNA3.1, and 0.025 μg of pRL-TK. Transfections were performed using the Lipo8000™ transfection reagent. After 24 h, the cells in each well were lysed with 100 μL of 1× Passive Lysis Buffer. Firefly and Renilla luciferase activities were measured separately for each sample using the Dual-Luciferase® Reporter Assay Kit. Promoter activities were quantified using a Luminoskan Ascent luminometer (Thermo, USA).

Confocal microscopy

For subcellular localization assay, ZFIN cells were cultured in microscopic dishes and transfected with GFP-tagged and ER-DsRed plasmids. After 24 h, cells were stimulated with B-DNA for an additional 12 h. Subsequently, cells were fixed with 4% paraformaldehyde (PFA) solution for 15 min. Nuclei were stained with DAPI staining solution. The stained cells were imaged using a confocal microscope system (Leica, Germany). For co-localization assay, ZFIN cells were co-transfected with plasmids encoding STING-Flag and DAPK3-GFP. Following a 24 h transfection period, cells were stimulated with B-DNA for an additional 12 h. The cells were then fixed, permeabilized, and blocked. Subsequently, cells were incubated separately with anti-Flag primary antibodies and Alexa Fluor 594-conjugated secondary antibodies. Imaging was performed using a Leica laser scanning confocal microscope.

Co-immunoprecipitation (co-IP) assay

Co-immunoprecipitation (Co-IP) experiments were performed to investigate protein-protein interactions. Briefly, ZFIN cells were seeded in 5 cm dishes and transfected with the indicated plasmids. Thirty-six hours post-transfection, cells were washed three times with PBS and then lysed on ice for 30 min using NP-40 lysis buffer supplemented with protease inhibitors. Cell lysates were centrifuged to collect the supernatants. These supernatants were incubated overnight at 4°C with anti-Flag or anti-GFP antibody-conjugated agarose beads. Finally, bound proteins were eluted from the beads by boiling in 2× SDS loading buffer for 10 min. Western blot analysis was performed using anti-Flag or anti-GFP antibodies to detect protein interactions. Additionally, due to the unavailability of specific zebrafish antibodies, the phosphorylation levels of DAPK3, STING, IKKα, and IKKβ were assessed using immunoprecipitation with a pan-phospho-serine/threonine/tyrosine antibody.

Ubiquitination assay

ZFIN cells were seeded in 5-cm dishes and co-transfected with Ub-HA (or K63-HA) and the indicated plasmids. After 24 h, cells were stimulated with B-DNA for an additional 12 h. Protein was extracted following lysis and centrifugation. Subsequently, the protein lysates were incubated with anti-GFP or anti-Flag antibody-conjugated agarose beads overnight at 4°C. Ubiquitination was then visualized by Western blot using an anti-HA antibody.

Native PAGE

ZFIN cells were co-transfected with IRF3-Flag and the indicated plasmids. After 24 h, cells were stimulated with B-DNA for an additional 12 h. Cell lysates were prepared and separated into two portions. One portion was analyzed by SDS-PAGE, and the other by native PAGE. Native PAGE assay was performed using an 8% acrylamide gel without SDS. The running buffer consisted of 25 mmol/L Tris-HCl (pH 8.4), 0.5% deoxycholate, and 192 mmol/L glycine. Electrophoresis was conducted on ice for 60 min at 35 mA. Proteins were then transferred to a nitrocellulose membrane (Millipore, USA) for immunoblotting. IRF3 dimerization was examined using an anti-Flag antibody.

Crystal violet staining and cell viability assay

In the *in vitro* infection experiment, ZFIN cells were seeded in 24-well plates and transfected with the indicated plasmids or siRNAs. After 24 h, the cells were infected with SVCV for 72 h. *In vivo* infection experiments were conducted using zebrafish embryos. Embryos were micro-injected with either DAPK3 morpholino (Mo-DAPK3) or DAPK3 mRNA. Following micro-injection, embryos were infected with SVCV at a titer of 10^4 $TCID_{50}$. At 72 hours post-infection (hpi), hatched embryos were homogenized, and the resulting homogenate was filtered through a 0.22 μm membrane filter. The resulting filtrate was then used to infect ZFIN cells for 72 h. For crystal violet staining, cells were fixed with 4% PFA for 15 min and stained with 1% crystal violet solution for 30 min. For the cell viability assay, cell viability was examined using the TransDetect® Cell Counting Kit (TransGene, China).

***In vitro* transcription of DAPK3 mRNA and microinjection**

DAPK3 mRNA was synthesized using the MAXIscript™ T7 Kit (Thermo Fisher Scientific, USA). One-cell stage zebrafish embryos were injected with 0.025 μg of DAPK3 mRNA or 0.025 μg of a scramble sequence (control). Six hours after microinjection, embryos were challenged with 1 mL of SVCV at a titer of 10^4 $TCID_{50}$. Zebrafish embryos generally hatched into larvae after 48 h of development. Following 72 h of infection, larvae morphology and survival rates were recorded and the expression of immune-related genes, inflammatory factors, and apoptosis-related genes was detected by qPCR and Western blot. The schematic diagrams of experimental design are detailed in Supplementary Figure S1.

Knockdown of DAPK3 in ZFIN cells and zebrafish embryos

Specific siRNAs targeting DAPK3 (si-DAPK3) were synthesized by GenePharma (China). ZFIN cells were

transfected with these siRNAs at a concentration of 1 μg per well using the HiPerFect transfection reagent. Transfection with a negative control (NC) siRNA served as a control. After 24 h, the cells were stimulated with B-DNA for an additional 12 h. qPCR and Western blot were performed to detect DAPK3 expression. The specific siRNA sequences used in this study are provided in Supplementary Table S1.

Splice-blocking morpholino oligonucleotides (Mos) targeting DAPK3 (Mo-DAPK3) and a standard control Mo (Mo-STD) were designed and synthesized by Gene Tools (USA). Mos were microinjected into one-cell stage zebrafish embryos at a dose of 4 ng for Mo-DAPK3 and 8 ng for Mo-STD (control group). Six hours after microinjection, embryos were challenged with 1 mL of SVCV at a titer of 10^4 $TCID_{50}$ for viral challenge. Following 72 h of infection, larvae morphology and survival rates were recorded and the expression of immune-related genes, inflammatory factors, and apoptosis-related genes was detected by qPCR and Western blot. The specific sequences of Mo-DAPK3 and Mo-STD used in this study are provided in Supplementary Table S1.

Statistical analysis

Statistical analysis was performed using GraphPad Prism v.8.0 and IBM SPSS Statistics v.27. For comparisons between two or three treatment groups, Student's *t*-test was used, with significance levels indicated as: *: $P<0.05$; **: $P<0.01$; ***: $P<0.001$. Data that did not satisfy assumptions of normality were analyzed using the Kruskal-Wallis (K-W) test. Statistical significance was indicated by letter labeling, with a *P*-value<0.05 considered significant. Different letters within bar charts denote significant differences between groups. The gray values of Western blots were quantified using ImageJ software. Data are presented as mean±standard deviation (SD) from at least three independent experiments, with one representative experiment shown.

RESULTS

Zebrafish DAPK3 is induced by stimulation with GCRV, SVCV, B-DNA, and Z-DNA

The phylogenetic tree showed that DAPK3 is conserved among different species (Supplementary Figure S2A). The GenBank IDs of the species were listed in Supplementary Table S3. Amino acid alignment indicated that the DAPK3 protein shared high homology among *D. rerio*, *C. idella*, and *H. sapiens* (Supplementary Figure S2B). Protein structure predicted by AlphaFold3 indicated that zebrafish DAPK3 contains a conserved serine/threonine protein kinase catalytic (STKc) domain and a tetratricopeptide repeat (TPR) domain (Supplementary Figure S2C, D).

To investigate the role of zebrafish DAPK3 in response to viral infection, qPCR was performed to examine *Dr*DAPK3 expression levels. Following SVCV infection, it was detectable in all tested tissues and ZFIN cells, with high expression observed at 72 h in the zebrafish liver and at 48 h in ZFIN cells (Figure 1A). Similarly, GCRV infection resulted in upregulation of DAPK3 in most tissues, with the highest relative expression detected in the intestine at 12 h and in ZFIN cells at 24 h post-infection (Figure 1B).

Consistently, B-DNA treatment resulted in an increase in DAPK3 expression, with the highest levels observed in the kidney at 72 h and in ZFIN cells at 24 h post-stimulation (Figure 1C). In response to Z-DNA stimulation, DAPK3 expression was induced across all tested tissues and ZFIN cells, with notably higher relative expression observed in the intestine at 6 h and in ZFIN cells at 48 h post-stimulation (Figure 1D).

DAPK3 binds to STING and promotes its phosphorylation

To elucidate the molecular mechanisms governed by the DAPK3-STING signaling axis in zebrafish, we employed B-DNA as an agonist in cellular stimulation experiments. B-DNA was selected because it is widely recognized as a canonical activator of the STING-mediated antiviral pathway (Ishikawa et al., 2009; Xu et al., 2017). First, zebrafish DAPK3 was primarily localized in the cytoplasm and distributed in both the endoplasmic reticulum (ER) and mitochondria (mito) (Figure 2A, B). B-DNA stimulation increased DAPK3 phosphorylation, which subsequently enhanced its interaction with STING, as demonstrated by co-IP and co-localization assays (Figure 2C–E). Thus, similar to mammals, zebrafish DAPK3 also participates in the antiviral response through a STING-dependent signaling pathway.

Additionally, molecular docking analysis revealed that the Ser21 and Thr87 sites of DAPK3 are critical for its interaction with STING (Figure 2F). DAPK3 increased the phosphorylation levels of STING following B-DNA stimulation (Figure 2G). To confirm this, we generated mutants at these sites (Figure 2H). The results showed that single-site mutants (Ser21 or Thr87) decreased phosphorylation of both DAPK3 and STING, while the double-site mutant exerted a stronger inhibitory effect on their phosphorylation (Figure 2I–2J). These findings indicated that zebrafish DAPK3 interacts with STING and promotes its phosphorylation depending on its Ser21 and Thr87.

DAPK3 recruits TRIM32 to catalyze K63-linked ubiquitination of STING

Ubiquitination modifications are crucial for controlling STING activity. Our results demonstrated that DAPK3 enhanced the ubiquitination level of STING (Figure 3A). However, since DAPK3 lacks E3 ubiquitin ligase activity, it likely relies on other E3 ligases to facilitate STING ubiquitination. TRIM32 is an E3 ubiquitin ligase for STING (Zhang, 2012). Co-IP assays showed that both DAPK3 and STING can bind to TRIM32 (Figure 3B). Furthermore, overexpression of DAPK3 increased the phosphorylation of TRIM32 (Figure 3C), which in turn promoted TRIM32-mediated K63-linked ubiquitination of STING (Figure 3D). In contrast, knockdown of DAPK3 inhibited the K63-linked ubiquitination catalyzed by TRIM32 (Figure 3E). These results indicate that, in addition to directly catalyzing the phosphorylation of STING, zebrafish DAPK3 can also enhance STING activity by activating TRIM32, which subsequently mediates K63-linked ubiquitination of STING.

DAPK3 activates IFN-I expression via the STING-TBK1-IRF3 axis

It is well-established that STING responds to pathogen infection through the IRF3-dependent IFN-I pathway and the NF-κB-dependent inflammatory pathway (Stempel et al., 2019). To confirm the downstream adaptors mediated by zebrafish DAPK3-STING interaction, co-IP assays were performed to examine the association between DAPK3 and key downstream proteins, including IKKα, IKKβ, p65, TBK1, and IRF3. TBK1 serves as the crucial kinase for activating IRF3, while IKKα and IKKβ are the key kinases for NF-κB (Häcker & Karin, 2006; Tanaka & Chen, 2012). The results

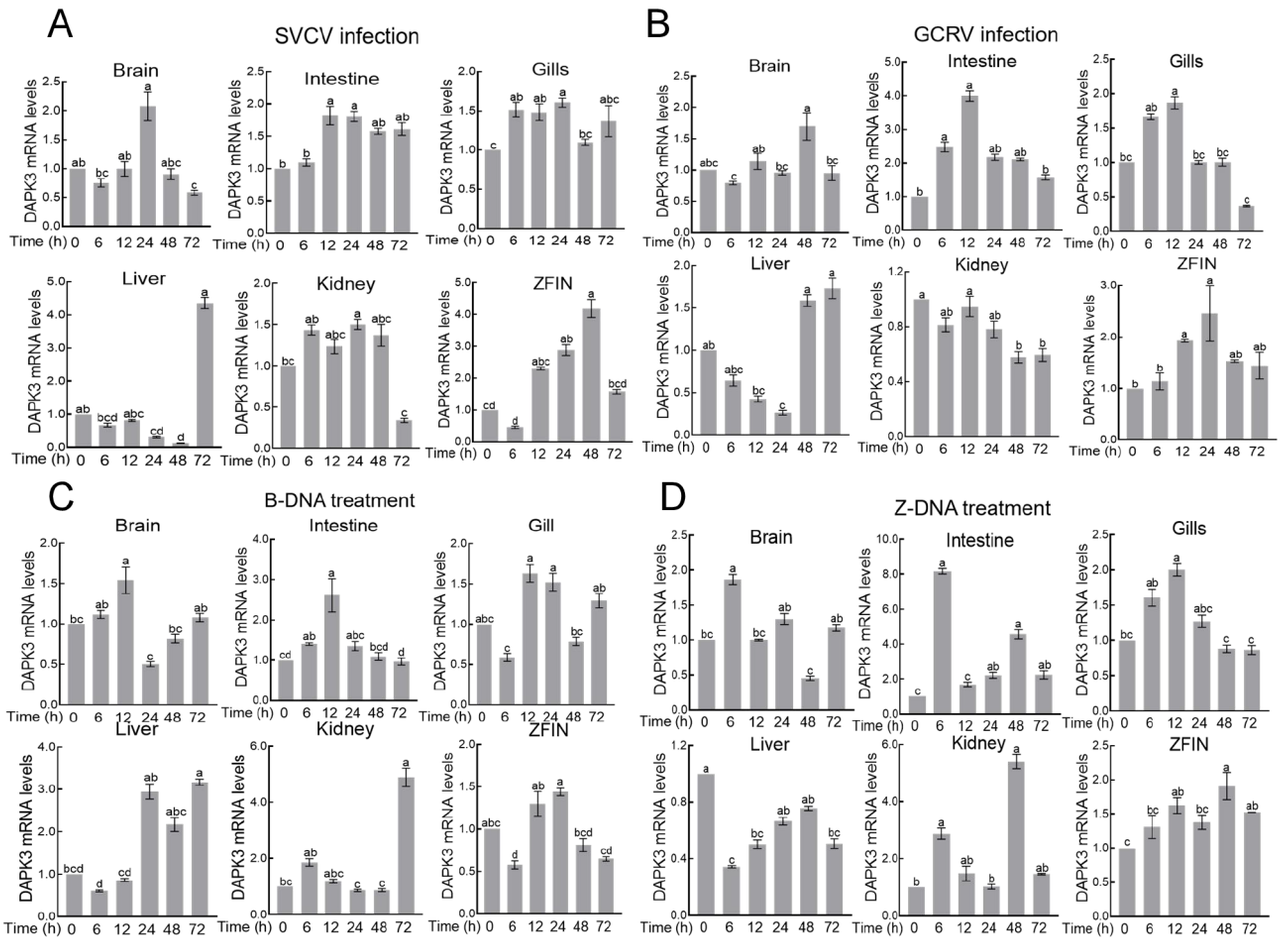


Figure 1 The expression of zebrafish DAPK3 is increased after stimulation with GCRV, SVCV, Z-DNA, and B-DNA in zebrafish or ZFIN cells

A–D: Zebrafish were separately injected with 10 μL of grass carp reovirus (GCRV) (10^6 $TCID_{50}$), 10 μL of spring viremia of carp virus (SVCV) (10^4 $TCID_{50}$), 2 μg of B-DNA, and 2 μg of Z-DNA. The mRNA was extracted from tested tissues (brain, gills, intestines, liver, and kidneys) at the indicated time points (6, 12, 24, 48, and 72 h). Meanwhile, ZFIN cells were separately treated with 10 μL of GCRV (10^6 $TCID_{50}$), 10 μL of SVCV (10^4 $TCID_{50}$), 2 μg of B-DNA, and 2 μg of Z-DNA. The 0 h group served as a control injected or treated with the same volume of PBS. The mRNA level of *DAPK3* was detected using qPCR. *β-actin* was used as the reference gene. The Kruskal-Wallis (K-W) test and Dunn's multiple comparisons were performed, and significant differences (P<0.05) were indicated by letter labeling. Data are based on one representative experiment performed in three biological replicates from at least three independent experiments (mean±SD).

indicated that DAPK3 interacts with IKKα, IKKβ, and TBK1 (Figure 4A). Therefore, zebrafish DAPK3 may also exert its antipathogenic functions by activating the STING-downstream IRF3-dependent type I interferon pathway and the NF-κB-dependent inflammatory pathway.

Primarily, we confirmed the role of DAPK3 in regulating the STING-TBK1-IRF3 axis. Knockdown of DAPK3 inhibited the interaction between STING and TBK1 (Figure 4B). The activated form (K63-linked ubiquitination and phosphorylation) of STING recruited the downstream kinase TBK1. TBK1 is a critical kinase for the IRF3-mediated IFN-I response (Fitzgerald et al., 2003). Dual-luciferase reporter assays demonstrated that overexpression of DAPK3 enhances IFN-I promoter activity (Figure 4C). DAPK3 overexpression increased both IFN-I expression and the phosphorylation levels of IRF3 and TBK1, while DAPK3 knockdown led to decreased IFN-I expression and reduced phosphorylation of IRF3 and TBK1 (Figure 4D, E). The effects of DAPK3 overexpression and knockdown were verified (Supplementary Figure S3A, B). qPCR analysis showed that DAPK3 augmented STING-induced expression of antiviral genes, including *Mxa, Mxb, Mxc* and *IFN-I* (Figure 4F). DAPK3 also enhanced the activity of STING downstream signaling components upon B-DNA stimulation, such as phosphorylated IRF3, phosphorylated TBK1, and IFN-I expression (Figure 4G), and promoted IRF3 dimerization (Figure 4H). Conversely, gene knockdown experiments produced consistent results, further confirming these findings (Figure 4I–4K). Collectively, these data suggest that zebrafish DAPK3 activates the STING-TBK1-IRF3 axis, leading to the induction of IFN-I.

DAPK3 enhances the canonical NF-κB pathway to induce apoptosis

Subsequently, we verified another role of DAPK3 in mediating the inflammatory response through the regulation of the STING-IKKα/IKKβ-NF-κB axis. Our results demonstrated that DAPK3 and STING synergistically increased the phosphorylation levels of IKKα and IKKβ (Figure 5A, B). Additionally, qPCR and WB assays indicated that DAPK3 promoted the production of inflammatory cytokines such as *IL-6*, IL-1β, and *TNFα*, as well as upregulated phosphorylation of p65 and the expression of TNFα (Figure 5C, D). Conversely,

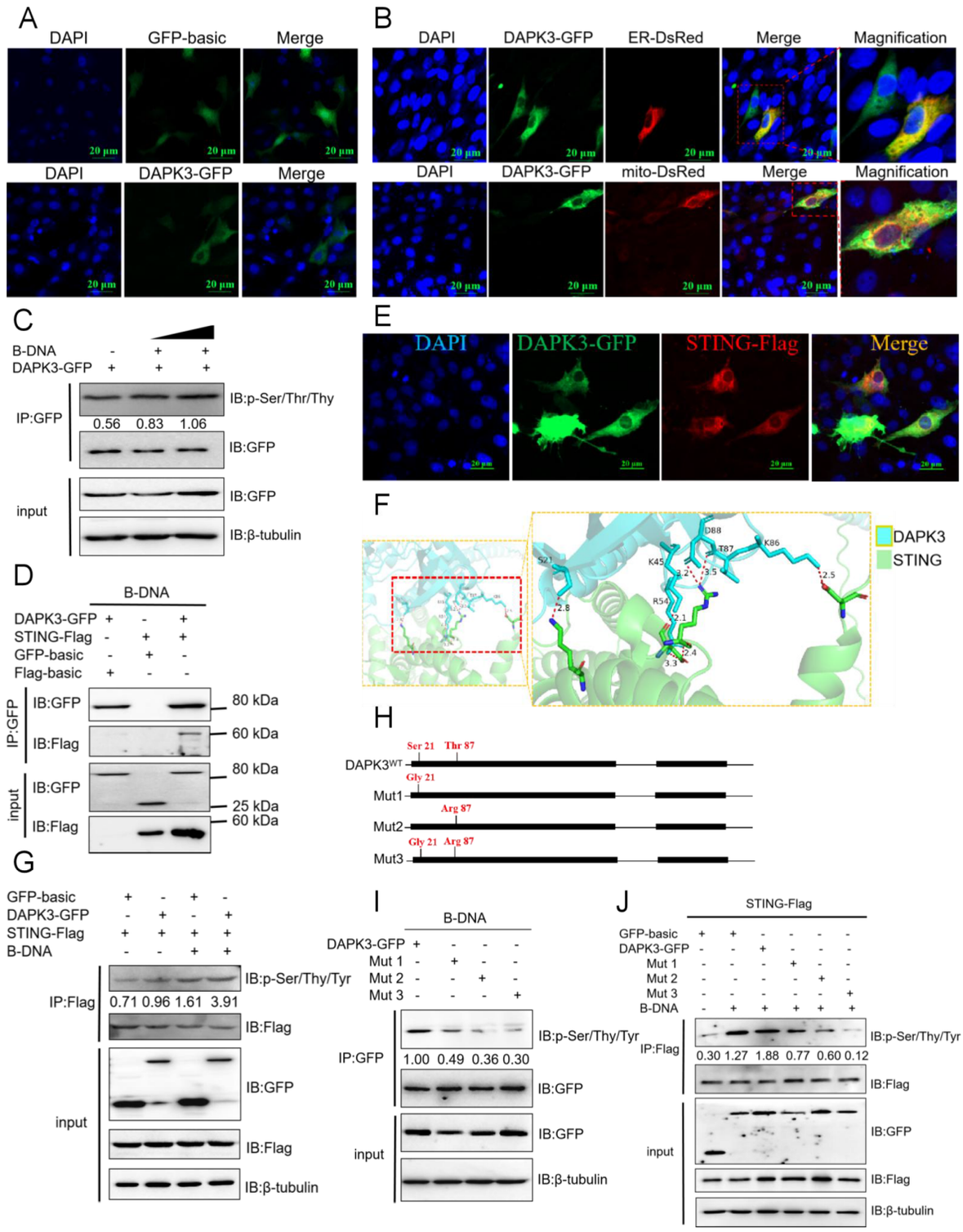


Figure 2 DAPK3 binds to STING and promotes its phosphorylation

A, B: ZFIN cells were separately transfected with GFP-basic, DAPK3-GFP, ER-DsRed, and mito-DsRed. After 12 h, the cells were stimulated with B-DNA for another 12 h. Subcellular localization analysis was performed. Scale bar: 20 μm. C: ZFIN cells were transfected with DAPK3-GFP. After 12 h, the cells were stimulated with B-DNA for another 12 h. Western blotting was used to detect phosphorylation of DAPK3. D, E: ZFIN cells were co-transfected with DAPK3-GFP and STING-Flag. After 24 h, the cells were stimulated with B-DNA for 12 h. Then, co-immunoprecipitation (co-IP) and co-localization assays were performed to detect the interaction. F: AlphaFold3 was used to predict the interaction sites between DAPK3 and STING. G: ZFIN cells were transfected with DAPK3-GFP and STING-Flag. After 24 h, the cells were stimulated with B-DNA for 12 h. STING phosphorylation was detected by co-IP assay using rabbit pan-phospho-serine/threonine/tyrosine antibody. H: Construction of DAPK3 mutants (Mut). I: ZFIN cells were separately transfected with DAPK3-GFP, Mut 1, Mut 2, and Mut 3. After 24 h, the cells were stimulated with B-DNA for 12 h. DAPK3 phosphorylation was detected by co-IP assay using rabbit pan-phospho-serine/threonine/tyrosine antibody. J: ZFIN cells were co-transfected with STING-Flag and DAPK3-GFP (or mutants). After 24 h, the cells were stimulated with B-DNA for 12 h. STING phosphorylation was detected by co-IP assay using rabbit pan-phospho-serine/threonine/tyrosine antibody.

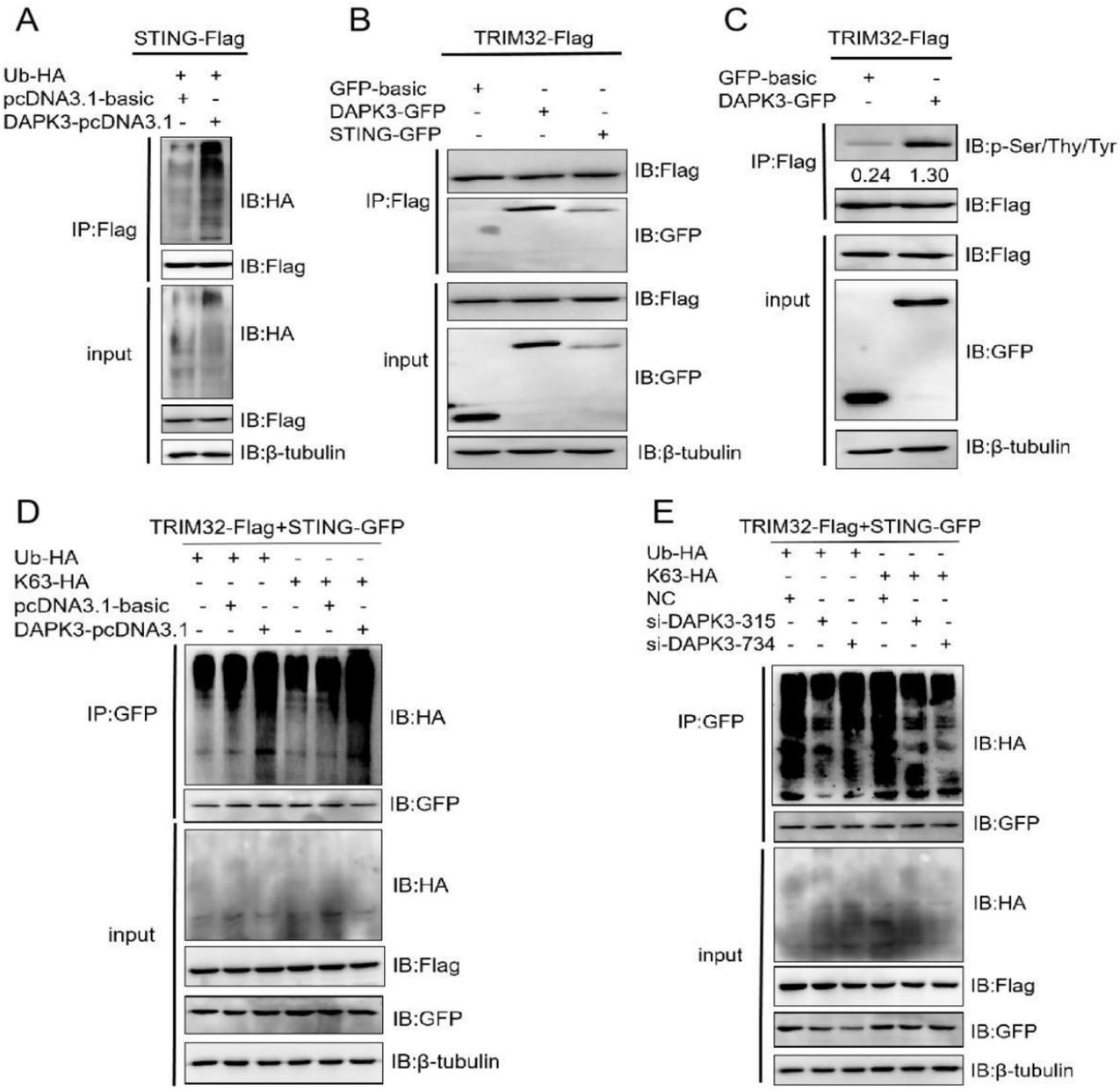


Figure 3 DAPK3 increases K63-linked ubiquitination of STING catalyzed by TRIM32

A: ZFIN cells were co-transfected with Ub-HA, STING-Flag, and DAPK3-pcDNA3.1. After 24 h, the cells were stimulated with B-DNA for 12 h. STING ubiquitination was detected by Western blot using anti-HA antibody. B: ZFIN cells were co-transfected with TRIM32-Flag and DAPK3-GFP (or STING-GFP). After 24 h, the cells were stimulated with B-DNA for 12 h. A co-IP assay was performed to examine the interaction between TRIM32-Flag and DAPK3-GFP (or STING-GFP). C: ZFIN cells were co-transfected with TRIM32-Flag and DAPK3-GFP. After 24 h, the cells were stimulated with B-DNA for 12 h. TRIM32 phosphorylation was detected. D, E: ZFIN cells were co-transfected with Ub-HA (or K63-HA), STING-GFP, TRIM32-Flag, and DAPK3-pcDNA3.1 (or si-DAPK3). After 24 h, the cells were stimulated with B-DNA for 12 h. STING ubiquitination was detected.

DAPK3 knockdown reduced p65 phosphorylation and decreased the production of these inflammatory factors (Figure 5E, F). Excessive production of inflammatory cytokines is often associated with apoptosis; consistent with this, our data showed that co-overexpression of DAPK3 and STING increased the expression of pro-apoptotic markers, including Bax, caspase-3, and caspase-9 (Figure 5G, H). Conversely, gene knockdown of DAPK3 resulted in similar reductions in these apoptotic markers (Figure 5I, J). These findings confirm that zebrafish DAPK3 enhances the STING-mediated canonical NF-κB pathway to induce inflammatory factor production and promote apoptosis.

In vivo overexpression of DAPK3 enhances resistance to SVCV infection

To investigate the antiviral role of DAPK3, SVCV was used in infection experiments because it is a pathogen to which zebrafish are highly susceptible (Liu et al., 2023; Wang et al., 2023). We first overexpressed DAPK3 in ZFIN cells infected with SVCV. Crystal violet staining and cell viability assays indicated that DAPK3 protected cells from SVCV infection (Figure 6A, B); qPCR and WB assays also found that DAPK3 decreased SVCV replication (Supplementary Figure S4). Additionally, DAPK3 mRNA was injected into zebrafish embryos, and overexpression was confirmed by qPCR and WB analysis (Figure 6C). Following SVCV challenge, the

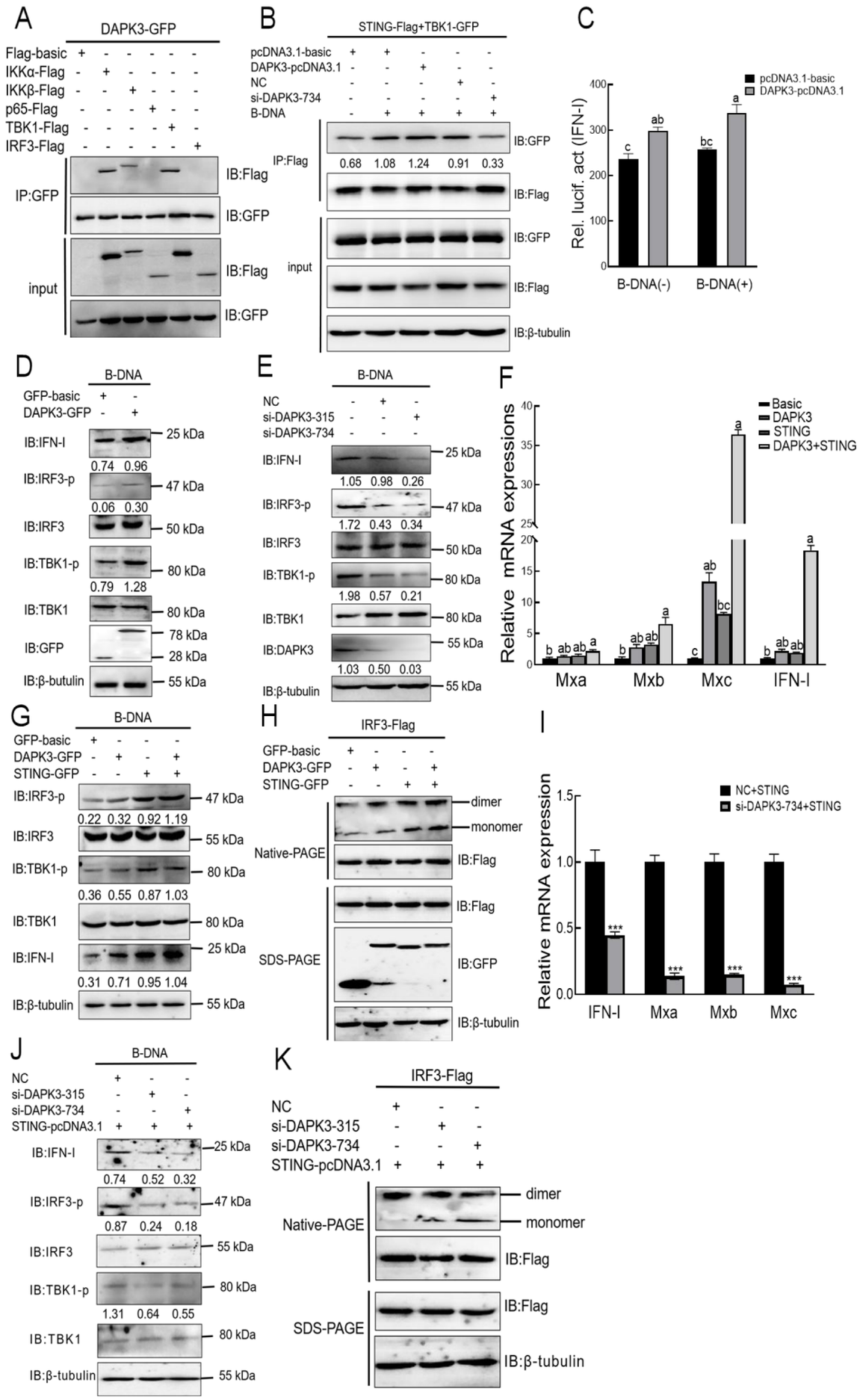

A
DAPK3-GFP
Flag-basic
IKKα-Flag
IKKβ-Flag
p65-Flag
TBK1-Flag
IRF3-Flag
IP:GFP
IB:Flag
IB:GFP
input
B
STING-Flag+TBK1-GFP
pcDNA3.1-basic
DAPK3-pcDNA3.1
NC
si-DAPK3-734
B-DNA
IP:Flag
IB:GFP
0.68 1.08 1.24 0.91 0.33
IB:Flag
input
IB:β-tubulin
C
pcDNA3.1-basic
DAPK3-pcDNA3.1
Rel. lucif. act (IFN-I)
B-DNA(-)
B-DNA(+)
D
B-DNA
GFP-basic
DAPK3-GFP
IB:IFN-I
25 kDa
0.74 0.96
IB:IRF3-p
47 kDa
0.06 0.30
IB:IRF3
50 kDa
IB:TBK1-p
80 kDa
0.79 1.28
IB:TBK1
80 kDa
IB:GFP
78 kDa
28 kDa
IB:β-butulin
55 kDa
E
B-DNA
NC
si-DAPK3-315
si-DAPK3-734
IB:IFN-I
25 kDa
1.05 0.98 0.26
IB:IRF3-p
47 kDa
1.72 0.43 0.34
IB:IRF3
50 kDa
IB:TBK1-p
80 kDa
1.98 0.57 0.21
IB:TBK1
80 kDa
IB:DAPK3
55 kDa
1.03 0.50 0.03
IB:β-tubulin
55 kDa
F
Basic
DAPK3
STING
DAPK3+STING
Relative mRNA expressions
Mxa
Mxb
Mxc
IFN-I
G
B-DNA
GFP-basic
DAPK3-GFP
STING-GFP
IB:IRF3-p
47 kDa
0.22 0.32 0.92 1.19
IB:IRF3
55 kDa
IB:TBK1-p
80 kDa
0.36 0.55 0.87 1.03
IB:TBK1
80 kDa
IB:IFN-I
25 kDa
0.31 0.71 0.95 1.04
IB:β-tubulin
55 kDa
H
IRF3-Flag
GFP-basic
DAPK3-GFP
STING-GFP
dimer
monomer
Native-PAGE
IB:Flag
SDS-PAGE
IB:GFP
IB:β-tubulin
I
NC+STING
si-DAPK3-734+STING
Relative mRNA expression
IFN-I
Mxa
Mxb
Mxc
J
B-DNA
NC
si-DAPK3-315
si-DAPK3-734
STING-pcDNA3.1
IB:IFN-I
25 kDa
0.74 0.52 0.32
IB:IRF3-p
47 kDa
0.87 0.24 0.18
IB:IRF3
55 kDa
IB:TBK1-p
80 kDa
1.31 0.64 0.55
IB:TBK1
80 kDa
IB:β-tubulin
55 kDa
K
IRF3-Flag
NC
si-DAPK3-315
si-DAPK3-734
STING-pcDNA3.1
dimer
monomer
Native-PAGE
IB:Flag
SDS-PAGE
IB:β-tubulin

Figure 4 DAPK3 positively regulates the IFN-I pathway via the STING-TBK1-IRF3 axis

A: ZFIN cells were co-transfected with DAPK3-GFP and one of the following recombinant plasmids (Flag-basic, IKKα-Flag, IKKβ-Flag, p65-Flag, TBK1-Flag, IRF3-Flag, STING-Flag). After 24 h, the cells were stimulated with B-DNA for 12 h. A co-IP assay was performed to examine their interaction. B: ZFIN cells were transfected with TBK1-GFP, STING-GFP, and DAPK3-pcDNA3.1 (or si-DAPK3). After 24 h, the cells were stimulated with B-DNA for 12 h. A co-IP assay was performed to examine the interaction intensity between TBK1 and STING. C: ZFIN cells were co-transfected with DAPK3-pcDNA3.1, pGL3-IFN-I-promoter, and pRL-TK. After 24 h, the cells were stimulated with B-DNA for 12 h. The activity of the IFN-I promoter was detected by dual-luciferase reporter assay. D, E: ZFIN cells were separately transfected with DAPK3-GFP and si-DAPK3. After 24 h, the cells were stimulated with B-DNA for 12 h. Western blotting was used to detect IFN-I, IRF3-p, IRF3, TBK1-p, TBK1, and DAPK3. F–H: ZFIN cells were transfected with STING and DAPK3. After 24 h, the cells were stimulated with B-DNA for 12 h. qPCR was used to detect the expression of *Mxa, Mxb, Mxc* and *IFN-I*. Western blotting was performed to examine the protein levels of IRF3-p, IRF3, TBK1-p, and IFN-I. Native PAGE assay was used to analyze IRF3 dimerization. I–K: ZFIN cells were transfected with si-DAPK3 and STING-pcDNA3.1. After 24 h, the cells were stimulated with B-DNA for 12 h. qPCR was used to detect the expression of *Mxa, Mxb, Mxc* and *IFN-I*. Western blotting was performed to examine the protein levels of IRF3-p, IRF3, TBK1-p, and IFN-I. Native PAGE assay was used to analyze IRF3 dimerization. Student's *t*-test was used, with significance levels indicated as: ***: $P<0.001$. The K-W test and Dunn's multiple comparisons were performed, and significant differences ($P<0.05$) were indicated by letter labeling. The gray scale of Western blots was calculated using ImageJ software. All data represent the results of three independent experiments.

morphology and survival rates of the embryos were monitored from 12 to 72 h post-infection. The results indicated that overexpression of DAPK3 had negligible effects on zebrafish larvae in the absence of infection; however, upon SVCV infection, it significantly increased survival rates compared to control injections of scramble sequences (Figure 6D, E). Viral titers, assessed by viral homogenate, revealed lower levels of cytopathic effects (CPEs) in the DAPK3-overexpressing group than in controls (Figure 6F). Furthermore, the overexpression of DAPK3 significantly augmented the expression of antiviral factors (*Mxa, Mxb*, Mxc, and *IFN-I*) and increased the phosphorylation of IRF3 and TBK1 upon SVCV infection (Figure 6G, H). In addition, inflammatory cytokines (*IL-6*, IL-1β, TNFα) and pro-apoptotic markers (*caspase-3*, caspase-9, Bax) were also upregulated in the DAPK3-overexpressing group after infection (Figure 6I–L). These findings are consistent with the results obtained from cell experiments. Collectively, *in vivo* data demonstrated that zebrafish DAPK3 functions as a positive regulator of the antiviral response.

Morpholino-mediated knockdown of DAPK3 impairs antiviral capability and inflammatory response of zebrafish larvae

To further confirm the antiviral role of DAPK3, we first knocked down DAPK3 in ZFIN cells, which resulted in significantly enhanced cytopathic effects (CPEs) and reduced cell survival (Figure 7A, B). Next, DAPK3 knockdown *in vivo* was performed by injecting Mo-DAPK3, and the efficiency was verified by qPCR and Western blot analysis (Figure 7C). DAPK3 knockdown significantly decreased larval survival rates following SVCV infection (Figure 7D, E). Viral titers, measured from samples injected with Mo-DAPK3, showed higher viral virulence compared to controls (Figure 7F). Furthermore, DAPK3 knockdown suppressed the expression of antiviral factors (*Mxa*, Mxb, Mxc, IFN-I) and reduced the phosphorylation levels of IRF3 and TBK1 upon SVCV infection (Figure 7G, H). Meanwhile, the expression of inflammatory cytokines (IL-6, IL-1β, TNFα) and pro-apoptotic factors (caspase-3, caspase-9, Bax) was also decreased in the DAPK3-knockdown group after infection (Figure 7I–L). These results reinforce the positive role of DAPK3 in the antiviral response.

In summary, these findings reveal a novel antiviral mechanism in zebrafish whereby DAPK3 promotes antiviral defense through STING-mediated induction of IFN-I production and initiation of the inflammatory response (Figure 8).

DISCUSSION

STING is a crucial adaptor protein in cytosolic viral nucleotide-triggered innate immunity in fish (Qin et al., 2025; Feng et al., 2014). Its protein levels and activity are precisely regulated by PTMs to effectively protect the host from infection and maintain immune homeostasis (Zhang et al., 2025). It has garnered considerable attention due to its central roles in regulating diverse cellular processes, including immune responses, inflammatory responses, and cancer progression (Barber, 2015). In this study, we identified zebrafish DAPK3 as a viral-responsive gene that positively regulates the antiviral response. DAPK3 is relatively conserved during evolution (Supplementary Figure S2) and can be induced by viral stimulation, including GCRV, SVCV, B-DNA, and Z-DNA. This suggests that zebrafish DAPK3 may be involved in both RNA- and DNA-induced immune responses and that DAPK3 is a typical antiviral factor (Figure 1). Interestingly, DAPK3 exhibited distinct spatiotemporal expression patterns in response to different agents, varying across organs, cell types, and time points. This differential expression may be due to variations in the intracellular signaling pathways triggered by each agent, even though they all commonly induce DAPK3 expression. The precise mechanisms underlying these agent-specific effects warrant further investigation.

In mammals, both the kinase activity and subcellular localization of DAPK3 are tightly regulated. DAPK3 translocates from the nucleus to the cytoplasm in response to extracellular stimuli, and its enzymatic activity is controlled by phosphorylation at key threonine and serine residues, such as Thr180, Thr225, and Ser50 (Bialik & Kimchi, 2006; Graves et al., 2005; Pike et al., 2008). The active form of DAPK3 significantly influences downstream signal transduction (Kawai et al., 1998; Park et al., 2024). We confirmed that zebrafish DAPK3 primarily localizes to the mitochondria and the endoplasmic reticulum, and that its phosphorylation level increases upon stimulation with B-DNA (Figure 2A, C), suggesting that B-DNA stimulation may induce DAPK3 autophosphorylation and trigger its activity. Interestingly, partial DAPK3 was observed in the nucleus, suggesting that its NLS sequences may be conserved between mammals and fish (Figure 2E). Subsequently, B-DNA stimulation promoted a specific interaction between DAPK3 and STING, leading to increased phosphorylation of STING (Figure 2D–G).

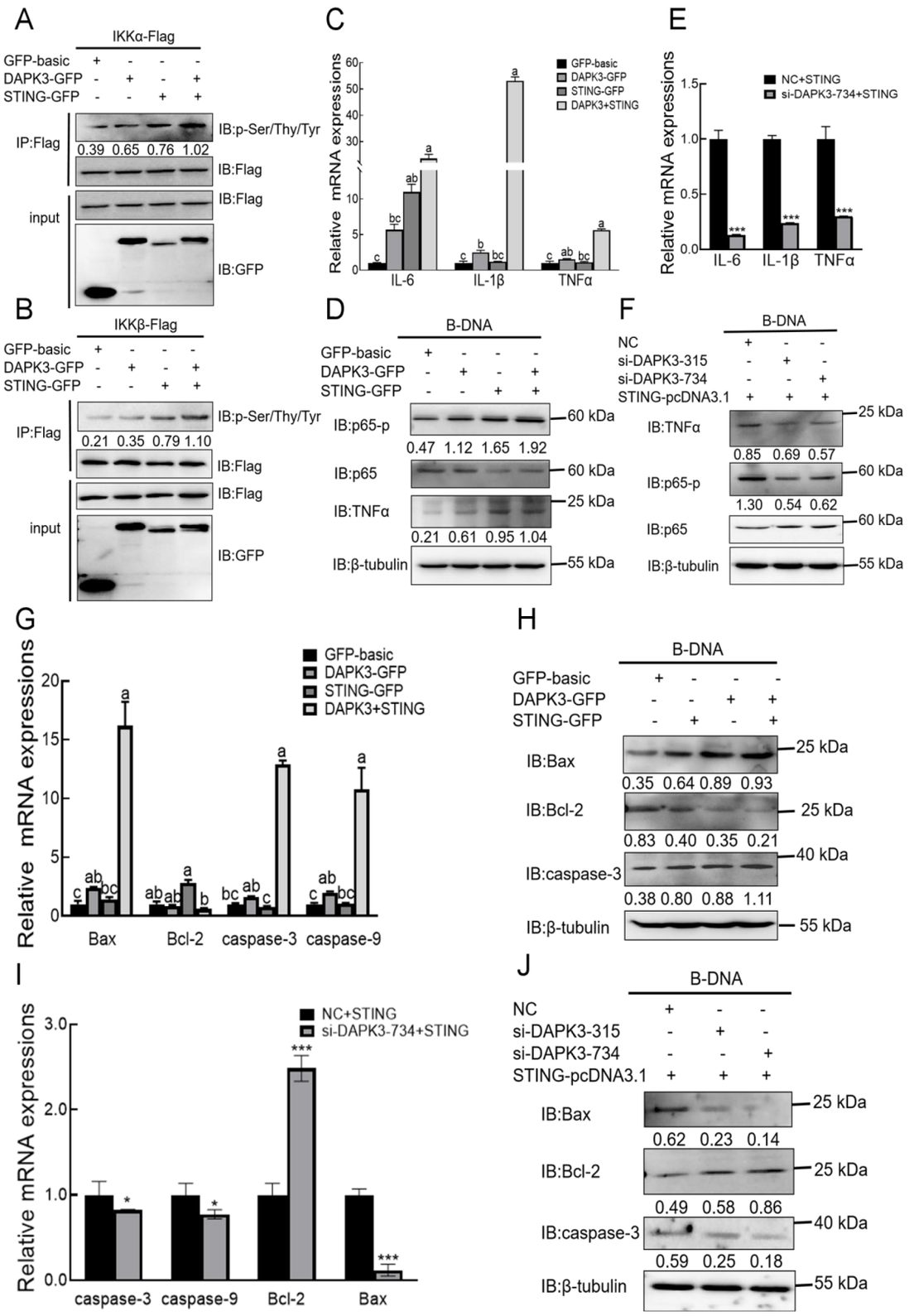


Figure 5 DAPK3 enhances the canonical NF-κB pathway to induce apoptosis

A, B: ZFIN cells were co-transfected with DAPK3-GFP, STING-GFP, and IKKα-Flag (or IKKβ-Flag). After 24 h, the cells were stimulated with B-DNA for 12 h. The phosphorylation of IKKα and IKKβ was detected by co-IP assay using a rabbit pan-phospho-serine/threonine/tyrosine antibody. C–F: ZFIN cells were transfected with DAPK3-GFP (si-DAPK3) and STING-GFP. After 24 h, the cells were stimulated with B-DNA for 12 h. qPCR was used to detect the mRNA levels of *IL-6*, IL-1β, and *TNFα*. Western blotting was performed to examine the protein levels of p65-p, p65, and TNFα. G–J: Apoptosis-related genes were also detected by qPCR and Western blotting, including Bax, Bcl-2, caspase-3, and caspase-9. Student's *t*-test was used, with significance levels indicated as: *: $P<0.05$; ***: $P<0.001$. The K-W test and Dunn's multiple comparisons were performed, and significant differences ($P<0.05$) were indicated by letter labeling. The grayscale of Western blots was calculated using ImageJ software. All data represent the results of three independent experiments.

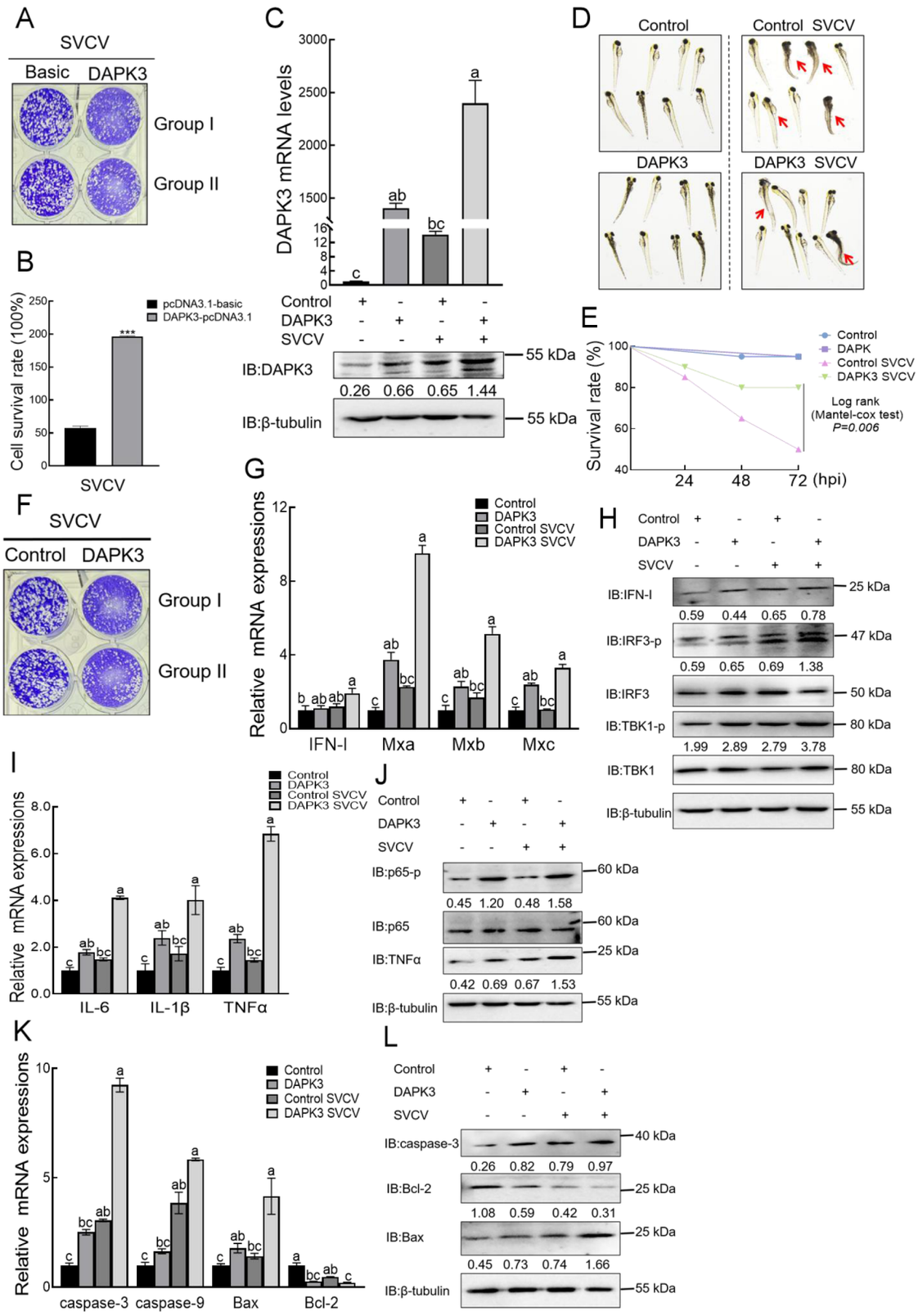


Figure 6 Overexpression of DAPK3 *in vivo* increases antiviral response in zebrafish

A, B: ZFIN cells were transfected with DAPK3-pcDNA3.1. After 12 h, the cells were infected with SVCV. Crystal violet staining and cell viability assays were performed. C: The overexpression of DAPK3 in zebrafish embryos was verified by qPCR and Western blot. D: The phenotype of zebrafish larvae after injection of DAPK3 mRNA; red arrows indicate dead individuals. E: The survival rate of zebrafish embryos. F: Homogenates from zebrafish embryos were used to infect ZFIN cells, and crystal violet staining was performed to analyze cytopathic effects. G, H: The expression of immune-related genes (IFN-I, Mxa, Mxb, Mxc, IRF3-p, TBK1-p). I, J: The expression of inflammatory factors (IL-6, IL-1β, TNFα, p65-p). K, L: The expression of apoptosis-related genes (caspase-3, caspase-9, Bax, Bcl2). Student's *t*-test was used, with significance levels indicated as: ***: $P<0.001$. The K-W test and Dunn's multiple comparisons were performed, and significant differences ($P<0.05$) were indicated by letter labeling. The gray scale of Western blot bands was calculated using ImageJ software. All data represent the results of three independent experiments.

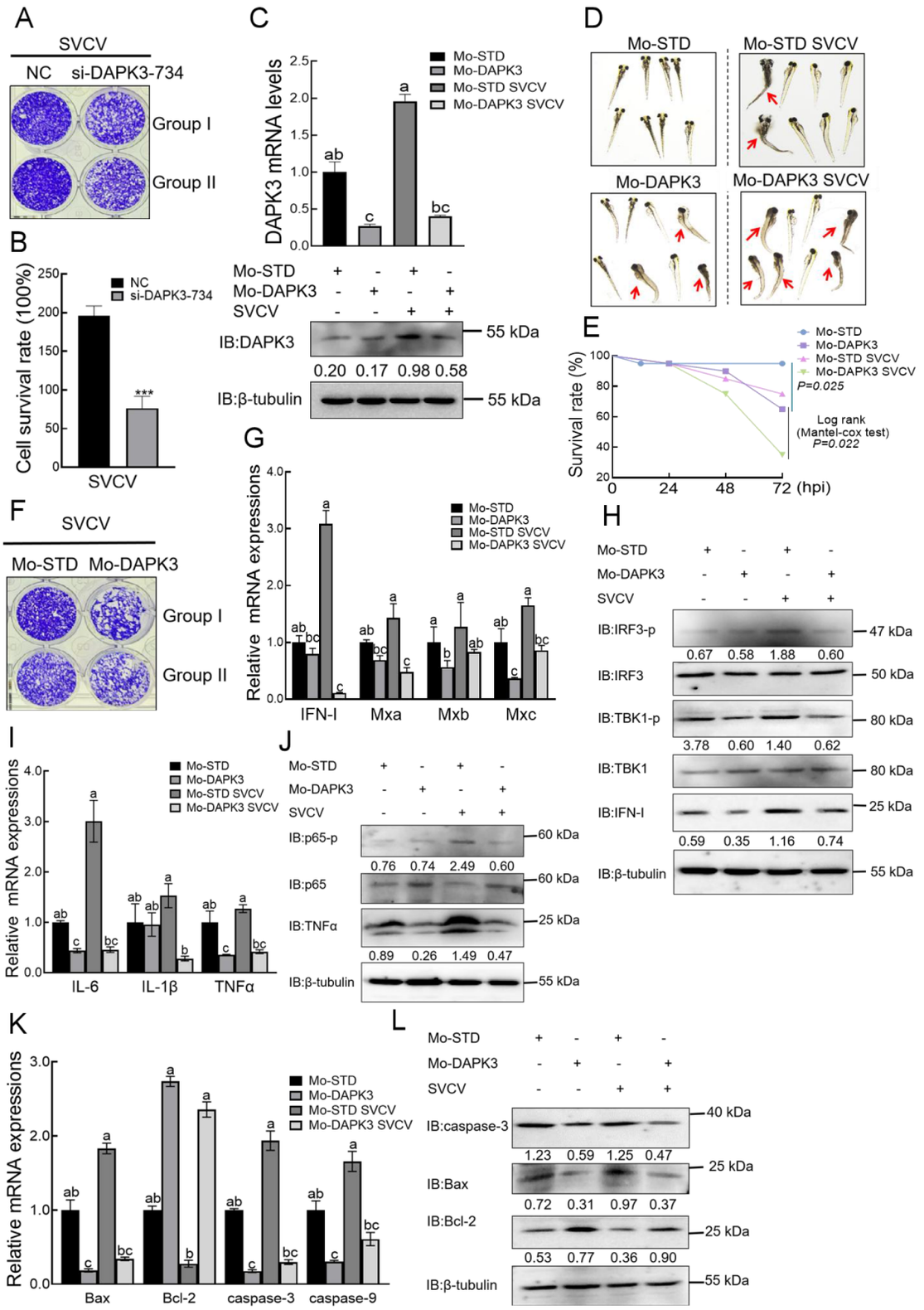


Figure 7 Knockdown of DAPK3 *in vivo* inhibits antiviral response in zebrafish

A, B: ZFIN cells were separately transfected with negative control (NC) and si-DAPK3-734. After 12 h, the cells were infected with SVCV. Crystal violet staining and cell viability assays were performed. C: The knockdown effect of DAPK3 in zebrafish embryos was verified by qPCR and Western blot. D: The phenotype of zebrafish larvae after injection of Mo-DAPK3; red arrows indicate dead individuals. E: The survival rate of zebrafish embryos. F: Homogenates from zebrafish embryos were used to infect ZFIN cells; crystal violet staining was performed to analyze cytopathic effects. G, H: The expression of immune-related genes (IFN-I, Mxa, Mxb, Mxc, IRF3-p, TBK1-p). I, J: The expression of inflammatory factors (IL-6, IL-1β, TNFα, p65-p). K, L: The expression of apoptosis-related genes (caspase-3, caspase-9, Bax, Bcl2). Student's *t*-test was used, with significance levels indicated as: ***: $P<0.001$. The K-W test and Dunn's multiple comparisons were performed, and significant differences ($P<0.05$) were indicated by letter labeling. The gray scale of Western blots was calculated using ImageJ software. All data represent the results of three independent experiments.

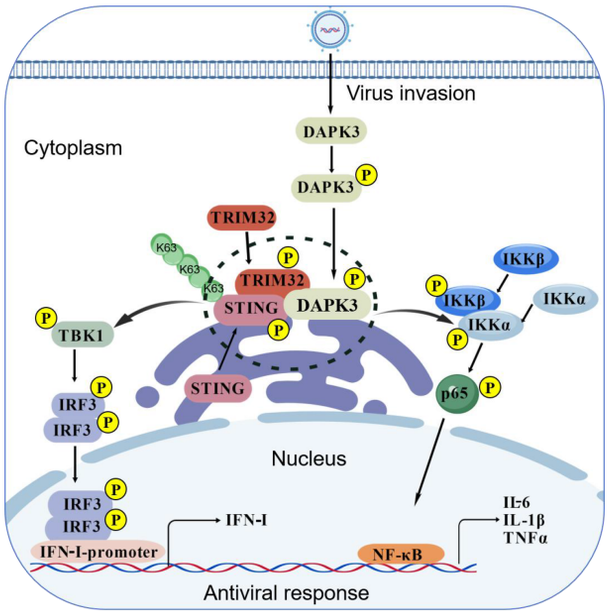


Figure 8 Schematic diagram of the work conducted in this study

Moreover, Thr87 and Ser21 residues of DAPK3 are responsible for STING interaction, because mutations at these sites impaired both DAPK3 and STING phosphorylation (Figure 2H–J). It is reported that the C-terminal tail region (CTT) of STING contains a highly conserved p-S-T-Y motif, where Ser/Thr phosphorylation serves as the core driver event for activation (Tsuchiya et al., 2016; Zhang et al., 2020). An increase in STING phosphorylation is a known indicator of its activated state. Zebrafish DAPK3 responds to B-DNA stimulation by localizing to mitochondria and the endoplasmic reticulum, forming an active conformation, and subsequently binding to STING to promote its phosphorylation. Consequently, zebrafish DAPK3 activates STING and its downstream signaling pathway.

Ubiquitination is a crucial post-translational modification that significantly impacts vital cellular activities by regulating the stability, activity, and localization of target proteins (Hershko & Ciechanover, 1998). It is known that K11- and K48-linked chains guide the substrate for proteasomal degradation, while K63- and M1-linked chains act as scaffolds for modifying proteins, thereby protecting protein activity. Meanwhile, the functions of the other four ubiquitin linkage types (K6, K27, K29, and K33) are being revealed gradually (Gao et al., 2023). STING activity is also regulated by ubiquitination. Numerous E3 ubiquitin ligases, such as RNF5, UBXN3B, TRIM32, and TRIM56, can modify the STING protein by attaching K48- or K63-linked ubiquitin chains, thereby mediating its degradation or activation, respectively (Deng et al., 2025; Kong et al., 2022; Yang et al., 2018). K63-linked ubiquitination is regarded to maintain the activity of substrate proteins (Gao et al., 2023; Lee et al., 2017; Madiraju et al., 2022).

In mammals, DAPK3 promotes STING ubiquitination by recruiting the E3 ubiquitin ligase LMO7 to STING (Takahashi et al., 2021). Our study reveals that DAPK3 promotes STING ubiquitination (Figure 3A), accompanied by its interaction—and that of STING—with the E3 ligase TRIM32 (Figure 3B). This is consistent with the reported localization of TRIM32 at the mitochondria and endoplasmic reticulum (Zhang et al., 2012), the primary sites of STING signaling. Thus, zebrafish DAPK3 recruits STING to TRIM32 at mitochondria and the endoplasmic reticulum. Furthermore, DAPK3 increases TRIM32 phosphorylation (Figure 3C), suggesting that DAPK3 enhances TRIM32 activity. Zebrafish DAPK3 enhances K63-linked ubiquitination of STING catalyzed by TRIM32 (Figure 3D, E). Therefore, in response to viral infection, unlike in mammals, zebrafish DAPK3 recruits TRIM32 to STING and forms a heterotrimer, thereby facilitating K63-linked ubiquitination and phosphorylation of STING. This K63-linked ubiquitination may in turn stabilize STING phosphorylation and sustain its activity. In the early stages of pathogen infection, STING activity is protected by phosphorylation and K63-linked ubiquitination, which is crucial for antiviral immune responses in fish. It is established that phosphorylation and ubiquitination modifications can synergistically regulate the same signaling pathway, thereby providing a mechanism for the fine-tuning of cellular responses and equipping cells with the ability to respond more effectively to diverse stimuli and environmental conditions (Filipčík et al., 2017).

To elucidate the downstream signaling of the DAPK3-STING axis in zebrafish, co-IP assays were performed to screen substrate proteins. Zebrafish DAPK3 interacted with TBK1 and the IKK complex (IKKα and IKKβ), whereas no association was detected with IRF3 or p65 (Figure 4A). IRF3, the interferon regulatory factor 3, is a key regulator for the activation of type I interferon expression (Huai et al., 2019). In mammals, phosphorylated STING recruits TANK-binding kinase 1 (TBK1), which subsequently phosphorylates IRF3 and induces IRF3-dependent IFNβ expression (Huang et al., 2011; Liu et al., 2015; Xu et al., 2010; Zhang et al., 2023b). On the other hand, the NF-κB-dependent inflammatory response is also a critical pathway targeted by STING, in which STING can directly interact with and phosphorylate the IKK complex (Abe & Barber, 2014). Thus, the zebrafish DAPK3-STING axis exerts antiviral capacity via the downstream IRF3-dependent IFN-I and NF-κB-dependent inflammatory pathways.

Subsequently, the zebrafish DAPK3-STING downstream IRF3-dependent IFN-I pathway was verified. Knocking down zebrafish DAPK3 inhibited the interaction between STING and TBK1. Zebrafish DAPK3 increased IFN-I expression, IRF3 and TBK1 phosphorylation levels, and IRF3 dimerization, ultimately leading to the production of Mx proteins (Mxa, Mxb, Mxc) and IFN-I (Figure 4). Upon invasion of the mammalian cytoplasm by microbial DNA from pathogens or self-DNA, STING recruits and activates TBK1. This activation increases IRF3's transcriptional activity via phosphorylation, leading to IRF3 homodimerization, nuclear translocation, and initiation of IFNβ production (Shu et al., 2014). Thus, the STING downstream IRF3-dependent IFN-I pathway is conserved in fish and mammals.

The IKK complex, comprising IKKα, IKKβ, and NEMO, is a well-established activator of the NF-κB pathway (Cruz et al., 2021; de Oliveira Mann et al., 2019). Upon activation, NF-κB (p50/p65) translocates to the nucleus, where it functions as a transcription factor to drive the expression of pro-inflammatory cytokines such as TNF-α, IL-1β, and IL-6 (Abdelnaser et al., 2024; Wan et al., 2020). In this study, the NF-κB-dependent inflammatory pathway is another downstream of the DAPK3-STING axis; zebrafish DAPK3 and STING increased the phosphorylation levels of both IKKα and IKKβ, as well as p65 phosphorylation and the expression of inflammatory factors (IL-6, IL-1β, and TNFα) (Figure 5A–F). Thus, the zebrafish DAPK3-STING complex directly activates the IKK complex

(IKKα and IKKβ) and promotes p65-dependent inflammatory factor expression. Similarly, mammalian DAPK3 has also been shown to activate the NF-κB signaling pathway, thereby promoting pro-inflammatory cytokine and chemokine production (Li et al., 2015). Furthermore, viral infection-induced inflammatory responses are known to activate cellular apoptosis, a mechanism that aids in clearing viral pathogens from infected host cells (Wang et al., 2011). Our results originally demonstrated that zebrafish DAPK3 and STING up-regulated the expression of apoptosis-related factors (Bax, caspase-3, caspase-9) (Figure 5G–J). Therefore, zebrafish DAPK3 can also activate the STING-dependent inflammatory response to defend against viral infection. In host cells, this elevated NF-κB activation may enhance the antiviral pressure exerted by the canonical type I IFN response (Balka et al., 2020; de Oliveira Mann et al., 2019).

To confirm the antiviral role of zebrafish DAPK3, DAPK3 was overexpressed or knocked down in ZFIN cells. The data indicated that DAPK3 prevented cell death and cytopathic effects (CPEs) from SVCV infection, and also decreased SVCV replication (Figure 6A, B; Supplementary Figure S4). Therefore, zebrafish DAPK3 is essential for host defense against SVCV infection. The antiviral role of DAPK3 also warrants *in vivo* verification. The zebrafish model, with its conserved signaling pathways and amenability to genetic manipulation, offers distinct advantages for dissecting immune-apoptotic crosstalk (Eimon & Ashkenazi, 2010). Viral pathogens such as spring viremia of carp virus (SVCV) and grass carp reovirus (GCRV) elicit IFN responses in zebrafish, mirroring mammalian antiviral defenses (Hong et al., 2023; Zhu et al., 2020). Consistent with our cellular findings, DAPK3 overexpression rescued zebrafish from SVCV infection, enhanced the expression of antiviral genes and inflammatory factors (Figure 6). Conversely, DAPK3 knockdown exacerbated SVCV-induced larval death, increased SVCV replication, and reduced the expression of antiviral genes and inflammatory factors (Figure 7).

Our data clarify a mechanism for the antiviral response of DAPK3 that is contingent upon its kinase activity, which triggers STING-dependent IRF3-mediated IFN-I and NF-κB-mediated inflammatory factor production. Nevertheless, it is worth differentiating the temporal activation of the IRF3- and NF-κB-dependent pathways by DAPK3 subsequent to SVCV infection in future studies.

CONCLUSION

This work uncovers a novel function of DAPK3 in the antiviral response, validated by both *in vitro* and *in vivo* models. Taken together, our findings demonstrate that zebrafish DAPK3 activates STING through phosphorylation and ubiquitination. This activation, in turn, triggers two parallel downstream pathways—the IRF3-dependent type I IFN response and the NF-κB-dependent inflammatory response—thereby enhancing host cell defense against viral infection.

SUPPLEMENTARY DATA

Supplementary data to this article can be found online.

COMPETING INTERESTS

The authors declare that they have no competing interests.

AUTHORS' CONTRIBUTIONS

T.T.Y.: Original draft writing, methodology, validation, investigation. C.Y.H.: Writing–review & editing, formal analysis. Q.L.Z.: Data curation. M.M.L.: Formal analysis. C.G.: Resources. M.F.L.: Data curation. L.H.F.: Resources. S.H.W.: Formal analysis. H.L.M.: Data curation. D.M.L.: Writing–review & editing. Z.Y.J.: Funding acquisition, conceptualization. X.W.X.: Writing–review & editing, project administration, funding acquisition, formal analysis, data curation, conceptualization. All authors read and approved the final version of the manuscript.

REFERENCES

Abdelnaser M, Alaaeldin R, Attya ME, et al. 2024. Modulating Nrf-2/HO-1, apoptosis and oxidative stress signaling pathways by gabapentin ameliorates sepsis-induced acute kidney injury. *Naunyn-Schmiedeberg's Archives of Pharmacology*, **397**(2): 947–958.

Abe T, Barber GN. 2014. Cytosolic-DNA-mediated, STING-dependent proinflammatory gene induction necessitates canonical NF-κB activation through TBK1. *Journal of Virology*, **88**(10): 5328–5341.

Balka KR, Louis C, Saunders TL, et al. 2020. TBK1 and IKKε act redundantly to mediate STING-induced NF-κB responses in myeloid cells. *Cell Reports*, **31**(1): 107492.

Barber GN. 2015. STING: infection, inflammation and cancer. *Nature Reviews Immunology*, **15**(12): 760–770.

Bialik S, Kimchi A. 2006. The death-associated protein kinases: structure, function, and beyond. *Annual Review of Biochemistry*, **75**: 189–210.

Cai ZQ, Cao R, Zhang K, et al. 2015. Oncogenic miR-17/20a forms a positive feed-forward loop with the p53 kinase DAPK3 to promote tumorigenesis. *Journal of Biological Chemistry*, **290**(32): 19967–19975.

Creagh EM, O'Neill LAJ. 2006. TLRs, NLRs and RLRs: a trinity of pathogen sensors that co-operate in innate immunity. *Trends in Immunology*, **27**(8): 352–357.

Cruz JA, Mokashi CS, Kowalczyk GJ, et al. 2021. A variable-gain stochastic pooling motif mediates information transfer from receptor assemblies into NF-κB. *Science Advances*, **7**(30): eabi9410.

Das TP, Suman S, Papu John AMS, et al. 2016. Activation of AKT negatively regulates the pro-apoptotic function of death-associated protein kinase 3 (DAPK3) in prostate cancer. *Cancer Letters*, **377**(2): 134–139.

de Oliveira Mann CC, Orzalli MH, King DS, et al. 2019. Modular architecture of the STING C-terminal tail allows interferon and NF-κB signaling adaptation. *Cell Reports*, **27**(4): 1165–1175. e5.

Deng CY, Chen DY, Yang L, et al. 2025. The role of cGAS-STING pathway ubiquitination in innate immunity and multiple diseases. *Frontiers in Immunology*, **16**: 1522200.

Du MJ, Chen ZJ. 2018. DNA-induced liquid phase condensation of cGAS activates innate immune signaling. *Science*, **361**(6403): 704–709.

Eimon PM, Ashkenazi A. 2010. The zebrafish as a model organism for the study of apoptosis. *Apoptosis*, **15**(3): 331–349.

Farag AK, Roh EJ. 2019. Death-associated protein kinase (DAPK) family modulators: current and future therapeutic outcomes. *Medicinal Research Reviews*, **39**(1): 349–385.

Feng XL, Yang CR, Zhang YX, et al. 2014. Identification, characterization and immunological response analysis of stimulator of interferon gene (STING) from grass carp *Ctenopharyngodon idella*. *Developmental & Comparative Immunology*, **45**(1): 163–176.

Filipčík P, Curry JR, Mace PD. 2017. When worlds collide-mechanisms at the interface between phosphorylation and ubiquitination. *Journal of Molecular Biology*, **429**(8): 1097–1113.

Fitzgerald KA, McWhirter SM, Faia KL, et al. 2003. IKKε and TBK1 are essential components of the IRF3 signaling pathway. *Nature Immunology*, **4**(5): 491–496.

Fujiwara N, Usui T, Ohama T, et al. 2016. Regulation of Beclin 1 protein phosphorylation and autophagy by protein phosphatase 2A (PP2A) and death-associated protein kinase 3 (DAPK3). *Journal of Biological*

Chemistry, **291**(20): 10858–10866.

Gao LY, Zhang W, Shi XH, et al. 2023. The mechanism of linear ubiquitination in regulating cell death and correlative diseases. *Cell Death & Disease*, **14**(10): 659.

Graves PR, Winkfield KM, Haystead TAJ. 2005. Regulation of zipper-interacting protein kinase activity in vitro and in vivo by multisite phosphorylation. *Journal of Biological Chemistry*, **280**(10): 9363–9374.

Guo C, Yu TT, Guo R, et al. 2026. Gpx4a-mediated ferroptosis underlines prothioconazole-induced ocular defects in early-life zebrafish. *Water Biology and Security*, **5**(4): 100512.

Häcker H, Karin M. 2006. Regulation and function of IKK and IKK-related kinases. *Science's STKE*, **2006**(357): re13.

Hershko A, Ciechanover A. 1998. The ubiquitin system. *Annual Review of Biochemistry*, **67**: 425–479.

Hong Y, Hu CB, Bai J, et al. 2023. Essential role of an ERV-derived Env38 protein in adaptive humoral immunity against an exogenous SVCV infection in a zebrafish model. *PLoS Pathogens*, **19**(4): e1011222.

Huai WW, Liu XG, Wang CM, et al. 2019. KAT8 selectively inhibits antiviral immunity by acetylating IRF3. *Journal of Experimental Medicine*, **216**(4): 772–785.

Huang YH, Huang XH, Yan Y, et al. 2011. Transcriptome analysis of orange-spotted grouper (*Epinephelus coioides*) spleen in response to Singapore grouper iridovirus. *BMC Genomics*, **12**(1): 556.

Ishikawa H, Ma Z, Barber GN. 2009. STING regulates intracellular DNA-mediated, type I interferon-dependent innate immunity. *Nature*, **461**(7265): 788–792.

Kawai T, Akira S. 2006. Innate immune recognition of viral infection. *Nature Immunology*, **7**(2): 131–137.

Kawai T, Matsumoto M, Takeda K, et al. 1998. ZIP kinase, a novel serine/threonine kinase which mediates apoptosis. *Molecular and Cellular Biology*, **18**(3): 1642–1651.

Kokkinidis M, Glykos NM, Fadouloglou VE. 2020. Catalytic activity regulation through post-translational modification: the expanding universe of protein diversity. *Advances in Protein Chemistry and Structural Biology*, **122**: 97–125.

Kong ZJ, Yin HY, Wang F, et al. 2022. Pseudorabies virus tegument protein UL13 recruits RNF5 to inhibit STING-mediated antiviral immunity. *PLoS Pathogens*, **18**(5): e1010544.

Lee BL, Singh A, Mark Glover JN, et al. 2017. Molecular basis for K63-linked ubiquitination processes in double-strand DNA break repair: a focus on kinetics and dynamics. *Journal of Molecular Biology*, **429**(22): 3409–3429.

Li J, Deng ZJ, Wang Z, et al. 2015. Zipper-interacting protein kinase promotes epithelial-mesenchymal transition, invasion and metastasis through AKT and NF-kB signaling and is associated with metastasis and poor prognosis in gastric cancer patients. *Oncotarget*, **6**(10): 8323–8338.

Liu RR, Meng F, Li X, et al. 2023. Characterization of STING from common carp (*Cyprinus carpio* L.) involved in spring viremia of carp virus infection. *Fish & Shellfish Immunology*, **142**: 109164.

Liu SQ, Cai X, Wu JX, et al. 2015. Phosphorylation of innate immune adaptor proteins MAVS, STING, and TRIF induces IRF3 activation. *Science*, **347**(6227): aaa2630.

Madiraju C, Novack JP, Reed JC, et al. 2022. K63 ubiquitination in immune signaling. *Trends in Immunology*, **43**(2): 148–162.

Pan J, Fei CJ, Hu Y, et al. 2023. Current understanding of the cGAS-STING signaling pathway: Structure, regulatory mechanisms, and related diseases. *Zoological Research*, **44**(1): 183–218.

Park JE, Park JW, Sim MK, et al. 2024. Inhibition of DAPK3 suppresses radiation-induced cellular senescence by activation of a PGC1α-dependent metabolism pathway in brain endothelial cells. *The Journals of Gerontology, Series A*, **79**(5): glae088.

Pike ACW, Rellos P, Niesen FH, et al. 2008. Activation segment dimerization: a mechanism for kinase autophosphorylation of non-consensus sites. *The EMBO Journal*, **27**(4): 704–714.

Qin XW, Li CR, Liang MC et al. 2025. RNF122 targets STING for ubiquitination at residues K95, K117, and K155 to regulate antiviral responses in a teleost fish. *Zoological Research*, **46**(4): 750–760.

Qin XW, Luo ZY, Pan WQ, et al. 2023. The interaction of mandarin fish DDX41 with STING evokes type I interferon responses inhibiting Ranavirus replication. *Viruses*, **15**(1): 58.

Qin Y, Wang M, Meng XT, et al. 2024. ISGylation by HERCs facilitates STING activation. *Cell Reports*, **43**(5): 114135.

Ru ZQ, Wu YT, Yang CY, et al. 2025. Ultra-short cyclic peptide CyRL-QN15 acts as a TLR4 antagonist to expedite oral ulcer healing. *Zoological Research*, **46**(5): 1187–1202.

Shu C, Li X, Li PW. 2014. The mechanism of double-stranded DNA sensing through the cGAS-STING pathway. *Cytokine & Growth Factor Reviews*, **25**(6): 641–648.

Shu HB, Wang YY. 2014. Adding to the STING. *Immunity*, **41**(6): 871–873.

Stempel M, Chan B, Juranić Lisnić V, et al. 2019. The herpesviral antagonist m152 reveals differential activation of STING-dependent IRF and NF-κB signaling and STING's dual role during MCMV infection. *The EMBO Journal*, **38**(5): EMBJ2018100983.

Su JG. 2025. Toll-like receptor signaling in teleosts. *Science China Life Sciences*, **68**(7): 1889–1911.

Sun JF, Yu HX, Wang YN, et al. 2023. Classical swine fever virus NS5A protein activates autophagy via the PP2A-DAPK3-Beclin 1 axis. *Journal of Virology*, **97**(12): e00988–23.

Takahashi M, Lio CWJ, Campeau A, et al. 2021. The tumor suppressor kinase DAPK3 drives tumor-intrinsic immunity through the STING-IFN-β pathway. *Nature Immunology*, **22**(4): 485–496.

Takaoka A, Wang ZC, Choi MK, et al. 2007. DAI (DLM-1/ZBP1) is a cytosolic DNA sensor and an activator of innate immune response. *Nature*, **448**(7152): 501–505.

Takeuchi O, Akira S. 2010. Pattern recognition receptors and inflammation. *Cell*, **140**(6): 805–820.

Tanaka Y, Chen ZJ. 2012. STING specifies IRF3 phosphorylation by TBK1 in the cytosolic DNA signaling pathway. *Science Signaling*, **5**(214): ra20.

Topham B, Hock B, Phillips E, et al. 2024. The role of innate priming in modifying tumor-associated macrophage phenotype. *Frontiers in Bioscience-Landmark*, **29**(12): 418.

Tsuchiya Y, Jounai N, Takeshita F, et al. 2016. Ligand-induced ordering of the C-terminal tail primes STING for phosphorylation by TBK1. *EBioMedicine*, **9**: 87–96.

Wan DS, Jiang W, Hao JW. 2020. Research advances in how the cGAS-STING pathway controls the cellular inflammatory response. *Frontiers in Immunology*, **11**: 615.

Wang WL, Hong JR, Lin GH, et al. 2011. Stage-specific expression of TNFα regulates bad/bid-mediated apoptosis and RIP1/ROS-mediated secondary necrosis in Birnavirus-infected fish cells. *PLoS One*, **6**(2): e16740.

Wang XL, Li ZC, Zhang C, et al. 2023. Spring viremia of carp virus N protein negatively regulates IFN induction through autophagy-lysosome-dependent degradation of STING. *The Journal of Immunology*, **210**(1): 72–81.

Xu D, Wei J, Cui H, et al. 2010. Differential profiles of gene expression in grouper *Epinephelus coioides*, infected with Singapore grouper iridovirus, revealed by suppression subtractive hybridization and DNA microarray. *Journal of Fish Biology*, **77**(2): 341–360.

Xu XW, Li MF, Wu Z, et al. 2017. Endoplasmic reticulum transmembrane proteins ZDHHC1 and STING both act as direct adaptors for IRF3 activation in teleost. *The Journal of Immunology*, **199**(10): 3623–3633.

Yang L, Wang LL, Ketkar H, et al. 2018. UBXN3B positively regulates

STING-mediated antiviral immune responses. *Nature Communications*, **9**(1): 2329.

Yang S, Yang Y, Xu LL, et al. 2025. DAPK3 is essential for DBP-induced autophagy of mouse Leydig cells. *Advanced Science*, **12**(17): 2413936.

Yang YH, Wen R, Yang N, et al. 2023. Roles of protein post-translational modifications in glucose and lipid metabolism: mechanisms and perspectives. *Molecular Medicine*, **29**(1): 93.

Zhang B, Xu PB, Ablasser A. 2025. Regulation of the cGAS-STING pathway. *Annual Review of Immunology*, **43**: 667–692.

Zhang C, Zhang SK, Kong FR, et al. 2023a. Ubiquitin C-terminal hydrolase L5 plays an essential role in the fly innate immune defense against bacterial infection. *Frontiers in Bioscience-Landmark*, **28**(11): 294.

Zhang J, Hu MM, Wang YY, et al. 2012. TRIM32 protein modulates type I interferon induction and cellular antiviral response by targeting MITA/STING protein for K63-linked ubiquitination. *Journal of Biological Chemistry*, **287**(34): 28646–28655.

Zhang LH, Zhang X, Liao JM, et al. 2023b. Grouper cGAS is a negative regulator of STING-mediated interferon response. *Frontiers in Immunology*, **14**: 1092824.

Zhang XW, Bai XC, Chen ZJ. 2020. Structures and mechanisms in the cGAS-STING innate immunity pathway. *Immunity*, **53**(1): 43–53.

Zhou BH, Hao QY, Liang YM, et al. 2023. Protein palmitoylation in cancer: molecular functions and therapeutic potential. *Molecular Oncology*, **17**(1): 3–26.

Zhu JJ, Liu X, Cai XL, et al. 2020. *Zebrafish prmt3* negatively regulates antiviral responses. *The FASEB Journal*, **34**(8): 10212–10227.